

1 Supplementary Material

2

3 Title: A combined morphometric and statistical approach to assess non- 4 monotonicity in the developing mammary gland of rats in the CLARITY-BPA 5 study

6
7 Maël Montévil^{1,3}, Nicole Acevedo^{1,4}, Cheryl M. Schaeberle^{1,5}, Manushree Bharadwaj², Suzanne E.
8 Fenton² and Ana M. Soto^{1,5}

9 ¹Department of Integrative Physiology and Pathobiology, Tufts University School of Medicine, Boston
10 MA 02111, USA

11 ²Division of the National Toxicology Program, NTP Laboratory, National Institute of Environmental
12 Health Sciences, Research Triangle Park, NC 27709, USA

13 Current Affiliations :

14 ³Institut de Recherche et d’Innovation, Centre Pompidou, Paris, France

15 ⁴Elavo Mundi Solutions, LLC, Minneapolis, MN 55406, USA

16 ⁵Department of Immunology, Tufts University School of Medicine, Boston MA 02111, USA
17

18 Corresponding author:

19 Ana M. Soto

20 Department of Immunology
21 Tufts University School of Medicine
22 136 Harrison Avenue
23 Boston, MA 02111
24 Phone (617) 636-6954
25 Email: ana.soto@tufts.edu

26
27
28 **Acknowledgments:** We would like to acknowledge the technical help provided by Dr. Luisa Camacho
29 and Dr. Barry Delclos regarding the generation of animals and the dissection of the mammary glands
30 examined in this study. We are also grateful to Dr. Barbara Davis for the histological assessment of the
31 lesions and to our colleagues at Tufts University, Dr. Carlos Sonnenschein and Dr. Beverly Rubin for
32 their critical reading of the manuscript. We thank Dr. Stuart Baker, (NCI) for useful suggestions about
33 the statistical design of this study. We are grateful to Dr. Marie Tremblay-Franco (section of Statistics
34 and Bioinformatics, Plateform MetaToul-AXIOM, INRA Toulouse) and Keith Shockley (NIEHS), for
35 their critical reading and useful suggestions regarding statistical analysis. This work was supported by
36 Grant Number U01ES020888, from the National Institute of Environmental Health Sciences (NIEHS;
37 A.M.S.) and NIEHS Funding 1Z01ES102785 (S.E.F. & M.B.). The content is solely the responsibility
38 of the authors and does not necessarily represent the official views of the NIEHS or the National
39 Institutes of Health.

40
41 **Declaration of competing financial interests:** The authors declare they have no actual or potential
42 competing financial interests.

43 **Supplementary analyses by PCA**

44 PCA is a method for dimensional reduction, i.e. for summarizing data sets where many quantities are
45 assessed simultaneously. The starting point of PCA is to build new quantities called dimensions (Dim,
46 named Dim 1, Dim 2, etc.) as linear combinations of the original quantities, for example if A, B, C are
47 quantities measured, $\text{Dim 1} = aA + bB + cC$ where a, b and c are determined by a computation. The new
48 quantities are built to be independent of each other and to explain as much of the variance as possible.
49 They are sorted by decreasing contribution to variance. The meaning of these dimensions with respect
50 to the original quantities is proper to a given dataset because the coefficients a, b, c, \dots are different for
51 different datasets. The strength of PCA is that it summarizes data in an automated fashion. Its limita-
52 tion is that properties not included in the first or first few dimensions may still be biologically relevant
53 (Section 7.5, Linear Algebra and Its Applications 5th Edition David C. Lay, Steven R. Lay, and Judi J.
54 McDonald Pearson 2014). As an example, the subtended area of a gland is correlated to many variables
55 since it is a way to assess the “size” of the gland, but the abundance of epithelial structures per unit vol-
56 ume conveys a different biological meaning. The latter can be more relevant to the understanding of
57 the effect of the treatment even though it can be independent of some “size” variations that dominate
58 spontaneous variability. As a result, the first dimension of PCA may not necessarily be of biological in-
59 terest when discussing the response to a treatment. Since the dimensions of PCA depend on the entire
60 data set, the results of PCA will be different depending on whether we include the positive controls
61 (0.5EE2 and 0.05EE2) in the analysis, see Figure S5.

62 **Table S1.** Semi-quantitative scoring guideline used for morphological assessment of PND 21 and PND
 63 90 mammary gland development in whole mounts following early life BPA or EE2 exposures.
 64

Age (PND)	Score	Criterion Used in Semiquantitative Scoring
21	1	Poor development, small epithelial growth, minimal branching and budding, few/no TEBs, poor development of cranial aspect of gland 4 (asymmetric)
	2	Gland almost reaches the lymph node (LN) (retarded growth), little branching or budding, few TEBs, poor development of cranial aspect of gland 4
	3	Gland touches LN, moderate branching and budding, external TEBs begin to appear around periphery, moderate development of cranial aspect of gland 4
	4	Gland touches LN, wide with equal antral and dorsal development (symmetric), internal and external TEBs, excellent branching and budding throughout gland, symmetric
	5	Excessive lateral growth, gland has grown past LN, dense budding with few gaps, internal and external TEBs, external TEBs around entire periphery
	6	Excessive lateral growth, growth beyond LN, 4th and 5th gland have grown together, dense budding with very few gaps, fewer TEBs because they are beginning to differentiate into lobules (looks like typical development on PND 35 or 50)
	7	Excessive lateral growth, gland has reached ends of fat pads and are terminally differentiating into lobules, 4th and 5th glands have grown over each other, very dense, difficult to see ducts (looks like young adult gland)
	1	Small gland that fails to fill fat pad, moderate number of TEBs remain, moderate branching and budding with large gaps, minimal to no lobules L1, poor left side development of 4 th gland (asymmetry)
	2	Small to medium gland growth, with several TEB remaining, moderate branching and budding, asymmetry remains, many lobules L1
	3	Medium sized gland with fair branching and growth, some TEBs, moderate budding with some gaps, small lobules L1-2. There is still some asymmetry of development
	4	Growth extends in both directions without reaching ends of fat pad, asymmetry is absent, gaps are evident, but branching and budding are moderate, more lobules L1-2 present
	5	Large gland almost reaching end of fat pad, few TEBs remain, dense branching, moderate budding with some gaps, many lobules L2-3
	6	Gland extended to ends of fat pad nearly everywhere, dense branching, few TEB remnants remain, budding throughout branches, developed lobules L3, some gaps remain
	7	Gland has reached ends of fat pad, terminally differentiated with no external or internal TEBs, dense branching and budding, no gaps, developed lobules L2-4, hard to see ducts

65
 66 Notes: PND=Postnatal Day, TEBs=Terminal End Buds, LN=Lymph Node, L=Lobule stage
 67 Lobule stage defined in Russo IH and Russo J. 1996. *Environ Health Perspect* 104:938-967.
 68

Table S2. Features measured by the automatic method applied to PND 21 mammary glands and complementary quantities used jointly in PCA and other analyses.

Type of analysis performed	Feature Label	Explanation of Feature Label
Weights	Necropsy Weight (g)	Body weight at necropsy (grams)
	Mammary Gland Weight (mg)	Weight of mammary gland (milligrams)
Manual assessment	TEB	Number of terminal end buds
Analyses of the 2D projection of the mammary tree	Area (μm^2)	Surface of 2D projection (square micrometers)
	Major (μm)	Size of the major axis of the gland (micrometers)
	Minor (μm)	Size of the minor axis of the gland (micrometers)
	Feret (μm)	Feret diameter (micrometers)
	AR	Aspect ratio of the gland
	Round	Roundness (inverse aspect ratio)
	Fractal Dimension	Self-explanatory (higher for denser glands, lower for sparse glands)
	Extension LV (μm)	Farthest distance from the lymph vessels (LV); negative when it is not reached (micrometers)
	Vesselp	Proportion of the gland beyond a specific lymph vessel
	Nodep	Proportion beyond the lymph node
Global analyses in 3D	Width (μm)	Width of the gland along its main directions (micrometers)
	Height (μm)	Height of the gland along its main directions (micrometers)
	Depth (μm)	Depth of the gland along its main directions (micrometers)
	Vol (μm^3)	Raw volume of epithelium (cubic micrometers)
	SA (μm^2)	Surface of the epithelium (i.e., surface the boundary epithelium/stroma) (square micrometers)
	Solidity 3D (μm^3)	Volume / convex volume (cubic micrometers)
	Encl Vol (μm^3)	Volume with some corrections (cubic micrometers)
	I1	Momentum of inertia along axis 1
	I2	Momentum of inertia along axis 2
	I3	Momentum of inertia along axis 3
	Euler	Assessment of Euler characteristic, which provides information on the lack of convexity of the object
	Holes	Number of topological holes.
	Thickness (μm)	Average local thickness of the gland (estimates the diameter, but biased by the compression exerted on the gland) (micrometers)
	SD Thickness (μm)	Average local thickness of the gland (estimates the diameter, but biased by the compression exerted on the gland) (micrometers)
	Max Thickness (μm)	Average local thickness of the gland (estimates the diameter, but biased by the compression exerted on the gland) (micrometers)
	Dimension 3D	Fractal dimension in 3D - high if the gland fills space in 3 dimension (thick, no lacunarity, high budding, ...)
Direct skeleton analysis (raw)	X Branches	Number of branches
	X Junctions	Number of junctions
	X Junction Voxels	Number of junction voxels
	Average Branch Length (μm)	Branch length (micrometers)

	X Triple Points	Number of bifurcation
	X Quadruple Points	Number of triple branching
	Maximum Branch Length (μm)	Maximum branch length (micrometers)
Direct skeleton analysis after pruning	X Branches1	Number of branches (only for non-terminal branches)
	X Junctions1	Number of junctions (only for non-terminal branches)
	X Junction Voxels1	Number of junction voxels (only for non-terminal branches)
	X Slab Voxels1	Number of voxels (only for non-terminal branches)
	Average Branch Length1 (μm)	Branch Length (micrometers) (only for non-terminal branches)
	X Triple Points1	Number of bifurcation (only for non-terminal branches)
	X Quadruple Points1	Number of triple branching (only for non-terminal branches)
	Maximum Branch Length1 (μm)	Maximum branch length (micrometers) (only for non-terminal branches)
Specialized analysis. When quantities are defined per branch the average over all branches is reported. All branches larger than 20μm are taken into account.	Size (μm)	Length of branch (micrometers)
	Number of Neighbors	Number of disregarded connections
	Depth from Root	Number of bifurcation from the nipple to the branch
	Depth Subtree (μm)	Average depth of the subtree of each branch (micrometers)
	Number of Children	Average number of sub branches
	Euclidean Distance (μm)	Distance between beginning and end of each branch (micrometers)
	Tortuosity	Ratio: length of branches /Euclidean distance
	Angle Between Beginning and End	Angle between beginning and end of a branch
	Angle with Parent Local	Angle between the end of the parent branch and the beginning the branch
	Angle with Parent Global	Angle between the direction of the parent branch and the branch
	Angle Wr Main Dir	Angle between the direction of the branch and the average direction of all branches
	Length to Nipple (μm)	Distance in the tree between a branch and the nipple (micrometers)
	Mean Width (μm)	Mean distance map of the branch without the z axis (i.e., 2D width of the branch) (micrometers)
	Max Width (μm)	Max distance map of the branch without the z axis (i.e., 2D width of the branch) (micrometers)
	SD Width (μm)	Standard deviation of the distance map of the branch without the z axis (i.e., 2D width of the branch) (micrometers)
	Mean Width2 (μm)	Mean local thickness of the branch (micrometers)
	Max Width2 (μm)	Max local thickness of the branch (micrometers)
	SD Width2 (μm)	Standard deviation of the local thickness of the branch (micrometers)
	Length Farthest Leaf (μm)	Distance in the tree between a branch and farthest leaf (micrometers)
	Topodepth	Total depth (number of bifurcation from nipple to the farthest branch)
	Nblarge	Putative bud clusters (structures with a wide end)
	Secondary Bud	Putative number of budding from ducts
	Nbbranchestree	Number of branches
	Type1 (%)	Percent secondary bifurcation
	Type2 (%)	Percent subbranches of secondary bifurcations
Specialized analysis. When quantities are	Size1 (μm)	Length of branches (micrometers)
	Number of Neighbours1	Number of disregarded connections

defined per branch the average over all branches is reported. Only branches larger than 75µm are taken into account.	Depth from Root1	Number of bifurcation from the nipple to the branch
	Depth Subtree1 (µm)	Average depth of the subtree of each branch (micrometers)
	Number of Children1	Average number of sub branches
	Euclidean Distance1 (µm)	Distance between beginning and end of each branch (micrometers)
	Tortuosity1	Ratio: length of branches /Euclidean distance
	Angle Between Beginning and End1	Angle between beginning and end of a branch
	Angle with Parent Local1	Angle between the end of the parent branch and the beginning the branch
	Angle with Parent Global1	Angle between the direction of the parent branch and the branch
	Angle Wr Main Dir1	Angle between the direction of the branch and the average direction of all branches
	Length to Nipple1 (µm)	Distance in the tree between a branch and the nipple (micrometers)
	Mean Width1 (µm)	Mean distance map of the branch without the z axis (i.e., 2D width of the branch) (micrometers)
	Max Width1 (µm)	Max distance map of the branch without the z axis (i.e., 2D width of the branch) (micrometers)
	SD Width1 (µm)	Standard deviation of the distance map of the branch without the z axis (i.e., 2D width of the branch) (micrometers)
	Mean Width2.1 (µm)	Mean local thickness of the branch (micrometers)
	Max Width2.1 (µm)	Max local thickness of the branch (micrometers)
	SD Width2.1 (µm)	Standard deviation of the local thickness of the branch (micrometers)
	Length Farthest Leaf1 (µm)	Distance in the tree between a branch and farthest leaf (micrometers)
	Topodepth1	Total depth (number of bifurcation from nipple to the farthest branch)
	Nblarge1	Putative bud clusters (structures with a wide end)
	Secondary Bud1	Putative number of budding from ducts
	Nbbranchestree1	Number of branches
	Type1.1 (%)	Percent secondary bifurcation
	Type2.1 (%)	Percent subbranches of secondary bifurcations

72 The table briefly describes the 91 structural features of mammary glands resulting from the automated
 73 method and three features assessed manually: animal weight, mammary gland weight and number of
 74 TEBs, represented in the top of the table. The left column provides a general description of the type of
 75 measurement, the “feature label” column refers to the way the feature is referred to in the text, and the
 76 “explanation of the feature label” column provides a succinct description of the feature. These features
 77 were used for the global analyses.

78 **Table S3.** Comparison of the test variable in the data, X_{observed} , and the statistics resulting from the
 79 permutation test for different values of the criteria A and B with datasets PND90CD, PND90SD,
 80 6MCD and 6MSD.

Criterion	X_{observed}	95 % of $X_{\text{sim}} <$	99 % of $X_{\text{sim}} <$	99.5% of $X_{\text{sim}} <$	$P_{\text{estimated}}$
A(1)=no threshold	1.43	1.08	1.24	1.29	0.00085***
A(1.05)	1.43	1.08	1.24	1.30	0.00091***
A(1.1)	1.49	1.09	1.26	1.32	0.00064***
A(1.2)	1.67	1.13	1.31	1.38	0.00016***
A(1.3)	1.66	1.15	1.34	1.41	0.00029***
A(1.4)	1.73	1.16	1.36	1.44	0.00026***
A(1.5)	1.93	1.17	1.32	1.45	2.2e-05***
A(1.75)	1.83	1.21	1.44	1.53	0.00029***
A(2)	1.55	1.23	1.47	1.56	0.0055**
A(2.5)	1.29	1.27	1.52	1.61	0.044*
B(1)=no threshold	1.24	1.11	1.27	1.33	0.014*
B(0.75)	1.25	1.10	1.27	1.33	0.012*
B(0.6)	1.29	1.11	1.28	1.34	0.0086**
B(0.5)	1.37	1.12	1.29	1.35	0.0038***
B(0.4)	1.36	1.14	1.32	1.39	0.0066**
B(0.3)	1.16	1.20	1.40	1.48	0.061
B(0.2)	1.31	1.26	1.50	1.59	0.037*
B(0.1)	1.41	1.47	1.81	1.95	0.060

81 **Note:** X is the test variable defined in the main text. X_{observed} , is the value of X observed in the data. X_{sim}
 82 is the distribution of X generated by the permutation test, under the H_0 hypothesis that all conditions
 83 are equivalent. $P_{\text{estimated}}$ is the p-value estimated for X_{observed} on the basis of X_{sim} . Number of animals per
 84 group n=8-10. Number of groups: 6.
 85

86 **Table S4.** Mean and standard deviation of conditions compared in the main text, in PND90CD,
 87 PND90SD, 6MCD and 6MSD. Number of animals per group n=8-10.
 88

Dataset	Quantity	Control	250BPA	0.5EE2
PND90CD	Average gland density	32.0 ± 14.1	18.1 ± 9.4	22.4 ± 7.0
PND90CD	Density in the rostral area (area 1)	36.6 ± 19.4	16.8 ± 12.03	28.6 ± 10
PND90CD	density in the middle of the gland (area 2)	27.1 ± 14.2	5.4 ± 17.6	11.9 ± 8.6
PND90CD	Lobuloalveolar budding	0.1 ± 0.32	0.9 ± 0.57	0.7 ± 0.67
PND90SD	lateral budding	1.3 ± 0.68	1.9 ± 0.57	2.4 ± 0.70
6MCD	fat pad area cm ²	41.1 ± 6.4	47.31 ± 5.4	44.2 ± 4.7
6MCD	percent coverage	52.2 ± 4.7	47.1 ± 4.5	57.4 ± 9.9
6MSD	standard deviation of gland density	6.58 ± 3.2	14.0 ± 7.3	8.2 ± 5.8
6MSD	percent coverage	52.4 ± 7.5	45.8 ± 4.9	53.2 ± 3.8
6MSD	Lateral branching	2.6 ± 0.52	2.0 ± 0	2.4 ± 0.52
6MSD	Lateral budding	1.6 ± 0.70	1.0 ± 0.47	1.8 ± 0.42
6MSD	alveolar budding	1.5 ± 0.85	0.6 ± 0.84	1.7 ± 0.82

89 **Note:** Control: vehicle control, EE2: ethinyl estradiol, BPA: bisphenol A. Units: $\mu\text{g}/\text{kg}$ body weight
 90 (bw)/day.

91 **Table S5.** Incidence of benign and malignant lesions/tumors identified from A) PND 90 and B) 6-
 92 month mammary glands following either continuous or stop-dose exposures across all treatment
 93 groups.

A

PND 90 Continuous Dose (PND90CD)

Treatment	Animals (n)	Lobular Hyperplasia	Fibroadenoma	Periductular Fibrosis (\pm lymphocytic infiltration)	Ductal epithelial necrosis with inflammatory infiltrate	DCIS
Control	10	0	0	0	0	0
2.5BPA	9	0	0	0	0	0
25BPA	10	0	0	1	0	0
250BPA	9	0	0	0	0	0
2500BPA	9	0	0	0	0	0
25000BPA	10	0	0	1	1	0
0.05EE2	10	0	0	0	0	0
0.5EE2	10	0	0	0	0	1

PND 90 Stop Dose (PND90SD)

Treatment	Animals (n)	Lobular Hyperplasia	Fibroadenoma	Periductular Fibrosis (\pm lymphocytic infiltration)	Ductal epithelial necrosis with inflammatory infiltrate	DCIS
Control	10	0	0	0	0	0
2.5BPA	8	0	0	0	0	0
25BPA	10	0	0	1	0	0
250BPA	10	0	0	0	0	2
2500BPA	8	0	0	0	0	0
25000BPA	10	0	0	0	0	0
0.05EE2	9	1	1	0	0	0
0.5EE2	10	0	0	0	0	0

94

B

6 Month Continuous Dose (6MCD)

Treatment	Animals (n)	Lobulo/Ductular-alveolar dilatation (\pm secretions)	Periductular Fibrosis (\pm lymphocytic infiltration)	Fibroadenoma	Adenoma	Adenocarcinoma (\pm cyst)
Control	10	0	1	0	0	0
2.5BPA	10	0	0	1	0	0
25BPA	10	0	0	1	0	0
250BPA	10	0	0	0	0	0
2500BPA	10	0	0	0	0	0
25000BPA	10	0	0	0	0	0
0.05EE2	10	0	0	0	0	0
0.5EE2	10	4	0	2	3	1

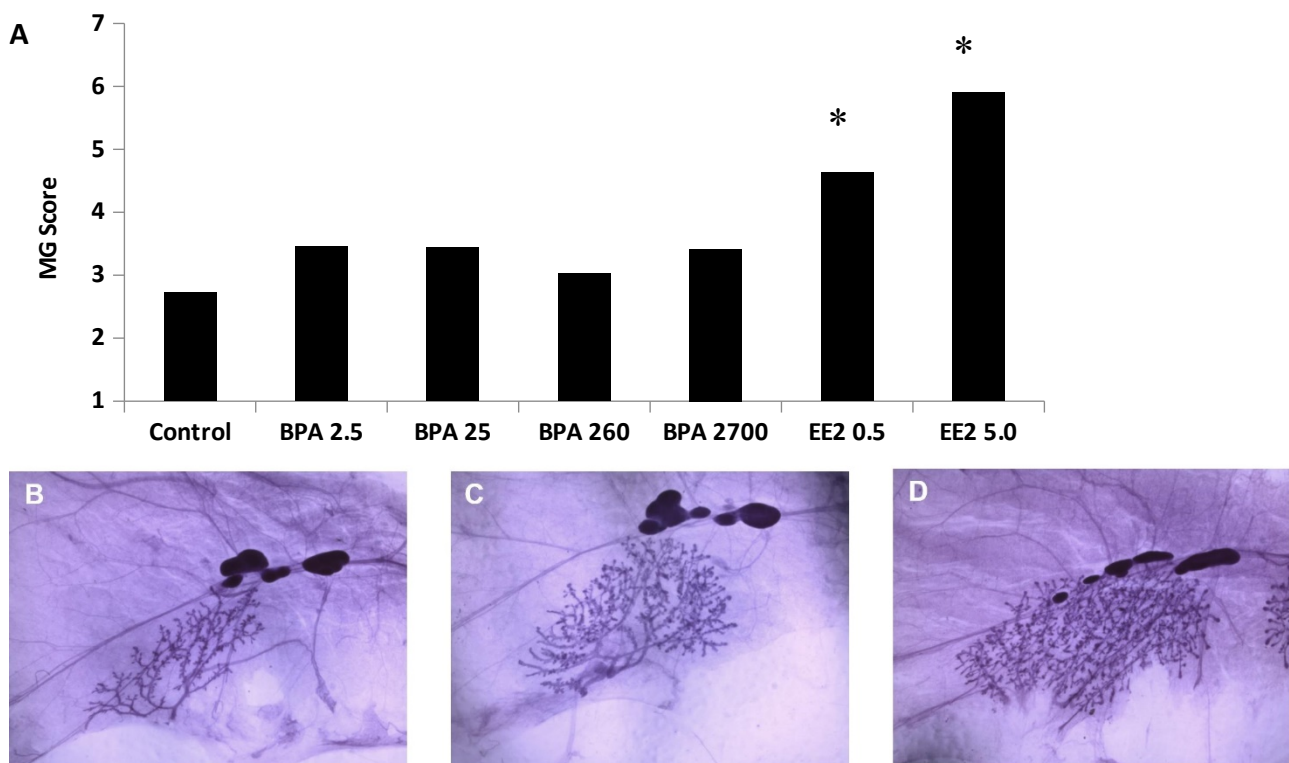
6 Month Stop Dose (6MSD)

Treatment	Animals (n)	Lobulo/Ductular-alveolar dilatation (\pm secretions)	Periductular Fibrosis (\pm lymphocytic infiltration)	Fibroadenoma	Adenoma	Adenocarcinoma (\pm cyst)
Control	10	0	0	0	0	0
2.5BPA	10	1	0	0	0	0
25BPA	10	0	0	0	0	0
250BPA	10	0	0	0	0	0
2500BPA	10	0	0	0	0	0

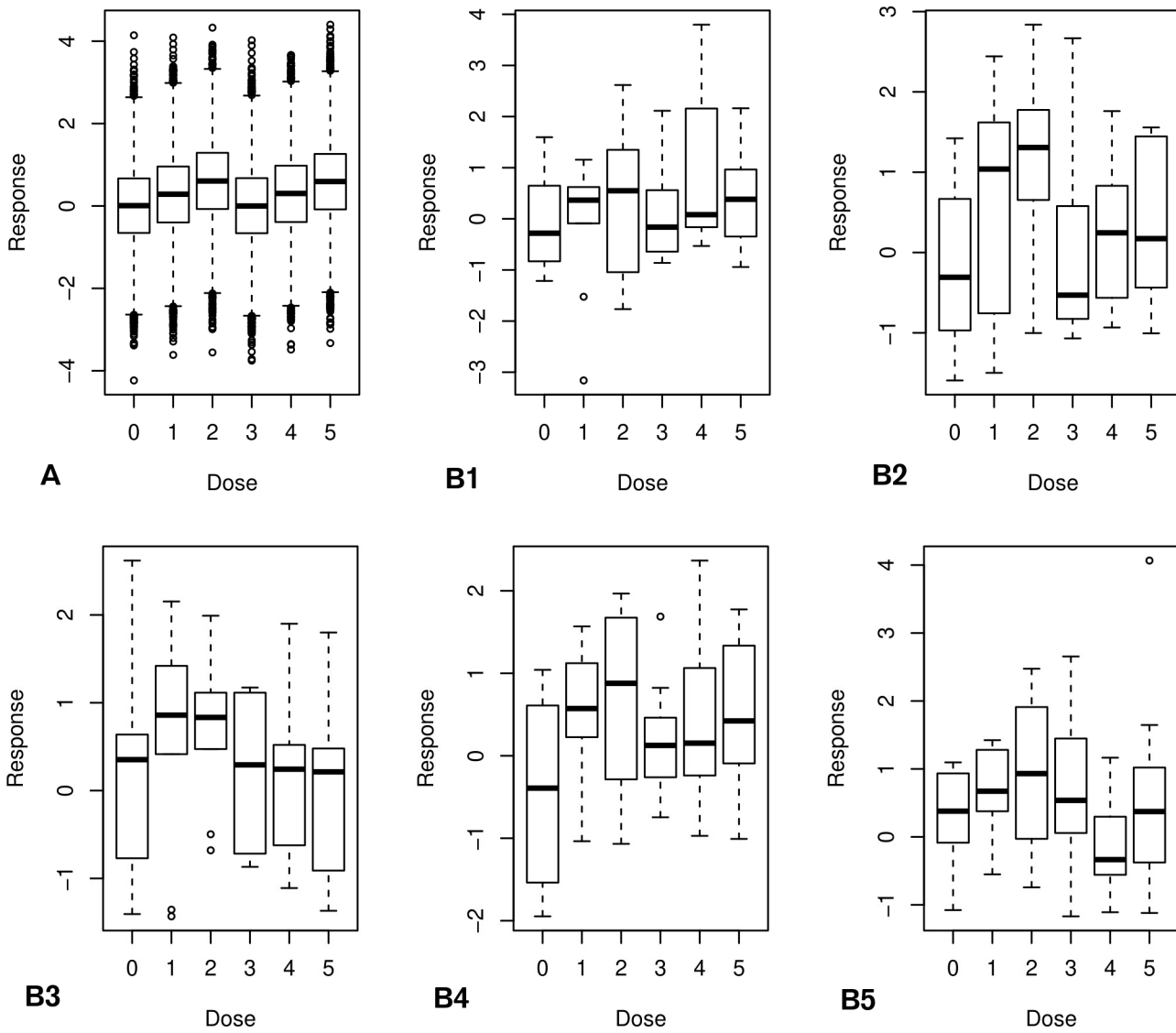
25000BPA	10	0	1	0	0	0
0.05EE2	10	0	0	0	0	0
0.5EE2	10	4	1	1	1	2

95 Note: Control: vehicle control, EE2: ethinyl estradiol, BPA: bisphenol A. Units: μg /kg body weight
 96 (bw)/day.

97
98
99
100
101
102
103



104
 105 **Figure S1: Scoring evaluation of PND21P mammary glands.** [A] Comparison of the mean semi-
 106 quantitative score of all treatment groups. Control: vehicle control, EE2: ethinyl estradiol, BPA:
 107 bisphenol A. Units: μg /kg body weight (bw)/day. Number of animals per group n=9-12. * indicates
 108 significantly accelerated gland development compared to vehicle controls (Kruskal Wallis; p=0.004
 109 and p<0.0001). Images are representative of mammary gland development in [B] PND21P vehicle con-
 110 trol group, [C] PND21P EE2 0.5 group, and [D] PND21P EE2 5.0 group.
 111
 112



113
114
115
116
117
118
119

Figure S2. Simulated dose response with $a=0.6$ (without correlations). The midline represents the median, the box represents the quartiles above and below the median and the whiskers represent the two other quartiles, excluding outliers. A: We represent a simulation with 10000 “animals” per group to show the shape of our simulated distribution. B: several iterations of our simulated distribution with the usual 10 animal per group.

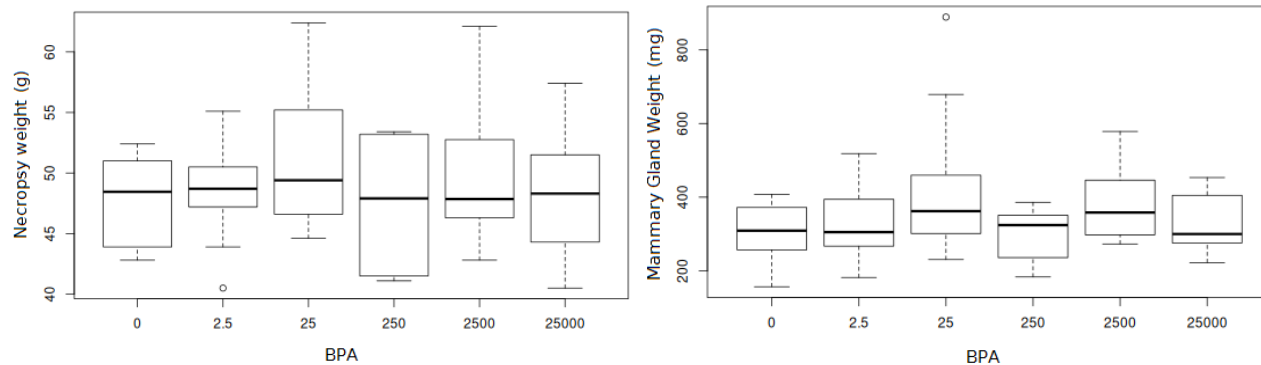


Figure S3. Effect of BPA on body weight and on mammary gland weight in PND21C. Control: vehicle control, BPA: bisphenol A. Units: $\mu\text{g}/\text{kg}$ body weight (bw)/day. The midline represents the median, the box represents the quartiles above and below the median and the whiskers represent the two other quartiles, excluding outliers. Number of animals per group n=8-10.

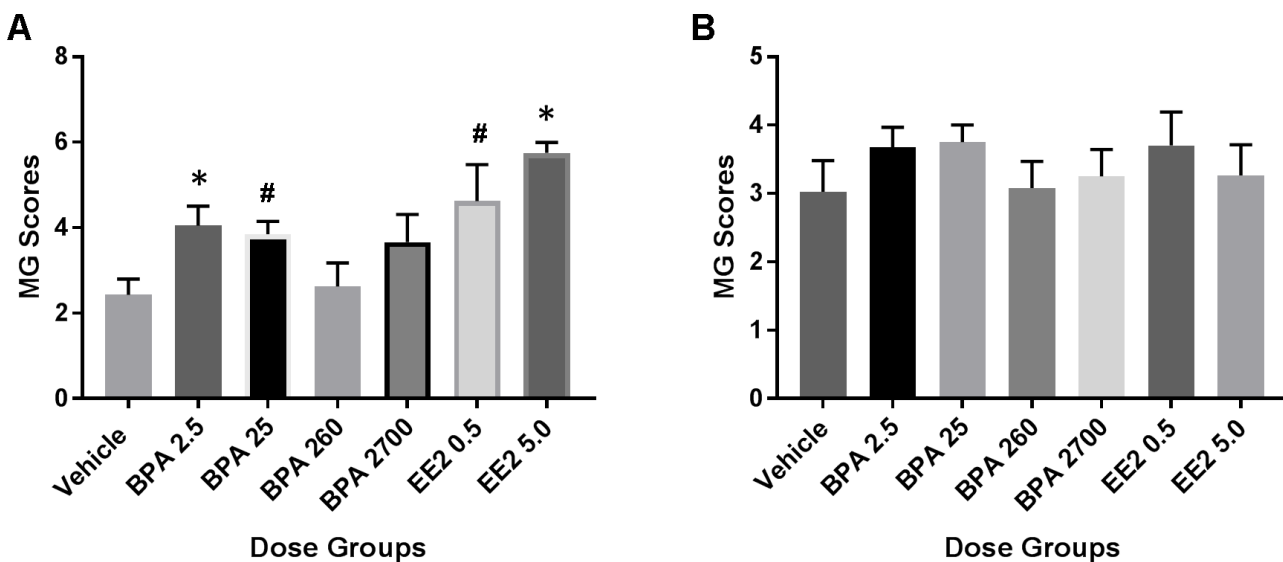
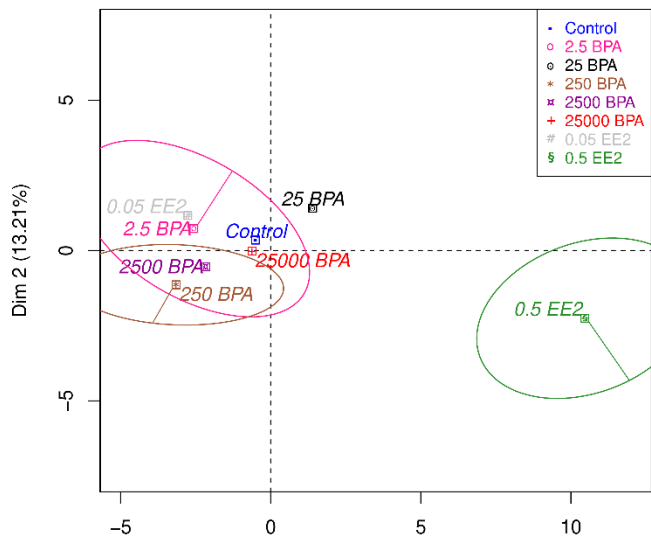
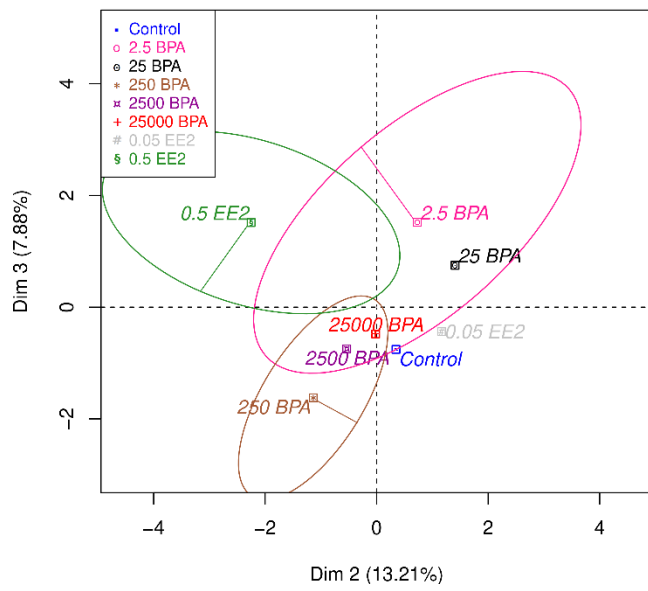


Figure S4. Semiquantitative scoring of postnatal day 90 pilot (PND90P) glands. Control: vehicle control, EE2: ethinyl estradiol, BPA: bisphenol A. Units: $\mu\text{g}/\text{kg}$ body weight (bw)/day. A) PND90P animals from Fenton group in which the majority of animals were in estrus at necropsy (only females in estrus included; n=7, 10, 10, 4, 6, 4, 4; from left to right). * Indicates significantly accelerated gland development compared to vehicle controls (Kruskal Wallis; BPA 2.5 p=0.05, EE5 p=0.01). # Indicates increased gland proliferation that did not reach significance (Kruskal Wallis; BPA 25 p=0.09, EE0.5 p=0.1). B) PND90P animals that were cycling from both Fenton and Soto groups, with all estrous cycle stages at necropsy included except anestrus (n=12, 18, 14, 10, 12, 12, 15, from left to right). All animals in A were included in B analysis.

A Individuals factor map (PCA)

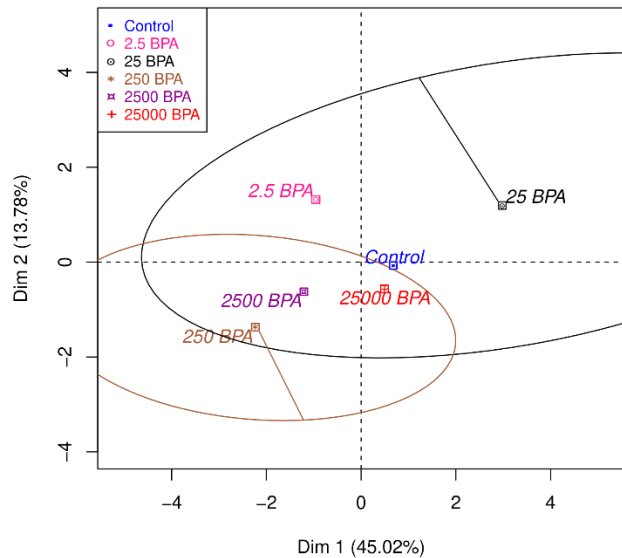
Dim 1 (47.17%)

B Individuals factor map (PCA)

Dim 2 (13.21%)

C

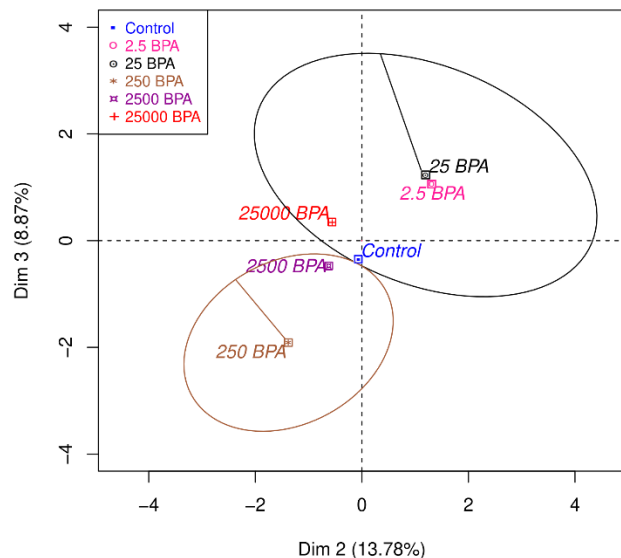
Individuals factor map (PCA)



Dim 1 (45.02%)

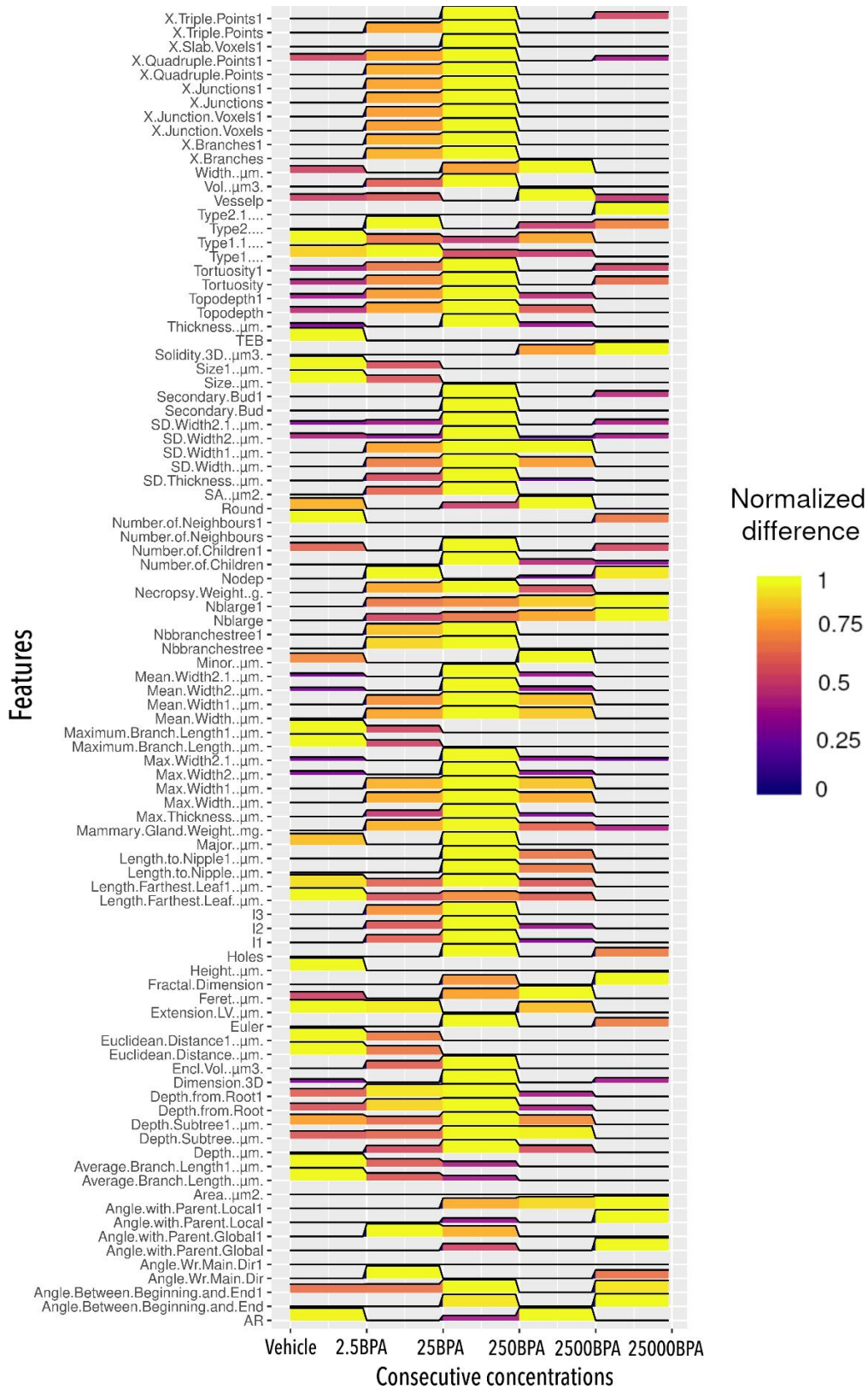
D

Individuals factor map (PCA)



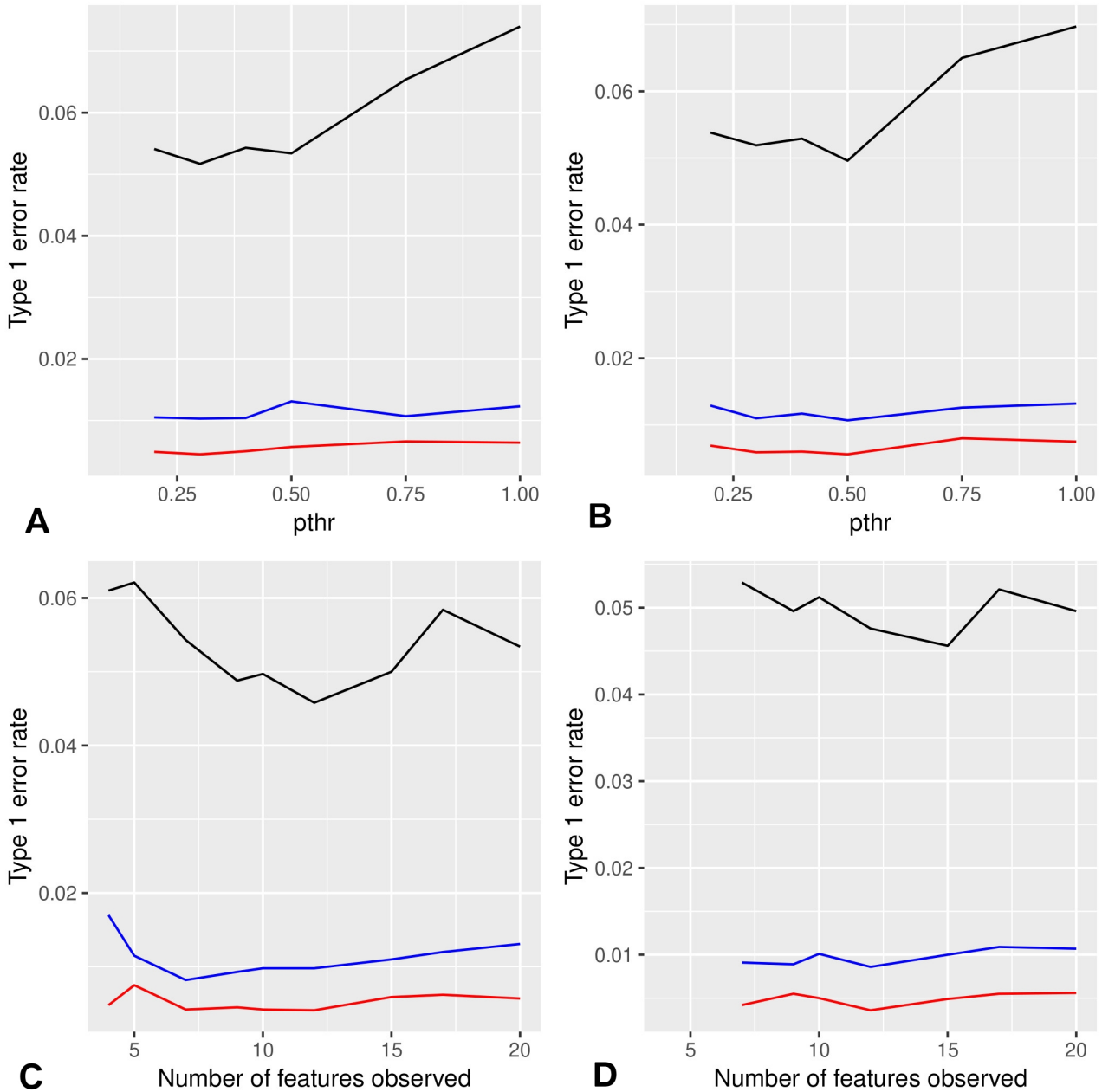
Dim 2 (13.78%)

Figure S5 Dimension 1 to 3 from PCA of PND21C animals with (top) and without (bottom) EE2 treatments. Control: vehicle control, EE2: ethinyl estradiol, BPA: bisphenol A. Units: $\mu\text{g}/\text{kg}$ body weight (bw)/day. We represent the average of each exposure group. Number of animals per group n=8-10.



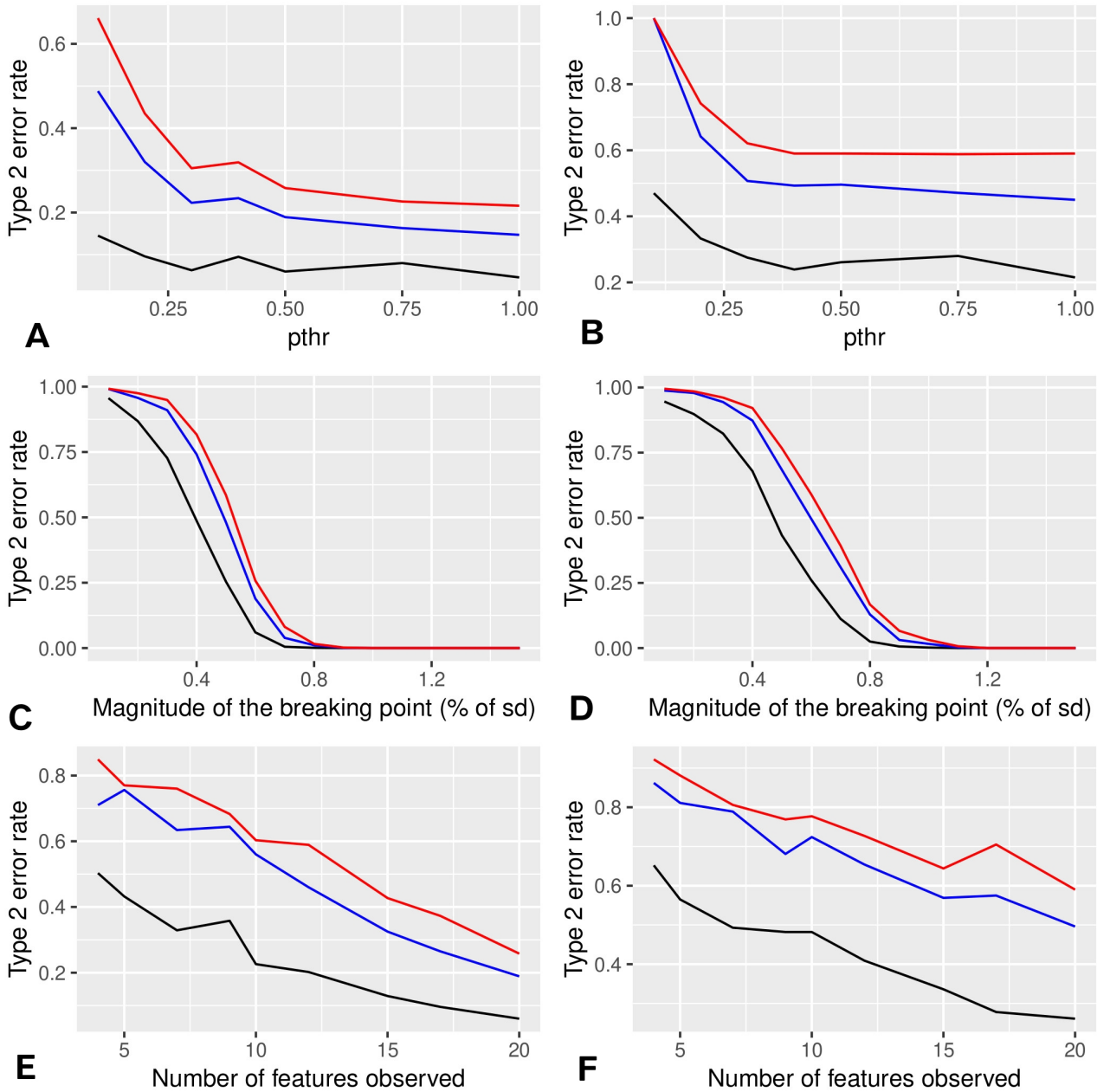
150

151 **Figure S6.** Comparison of the changes between consecutive doses for the 94 features in PND21C
 152 described in Table S 2. Vehicle: vehicle control, BPA: bisphenol A. Units: $\mu\text{g}/\text{kg}$ body weight
 153 (bw)/day. Largest consecutive changes meeting criterion B(0.5) for each observed feature in PND21C.
 154 All consecutive differences are normalized to a maximum of 1, in yellow. No data means that the
 155 criterion B(0.5) is not met for a given feature and consecutive concentration.



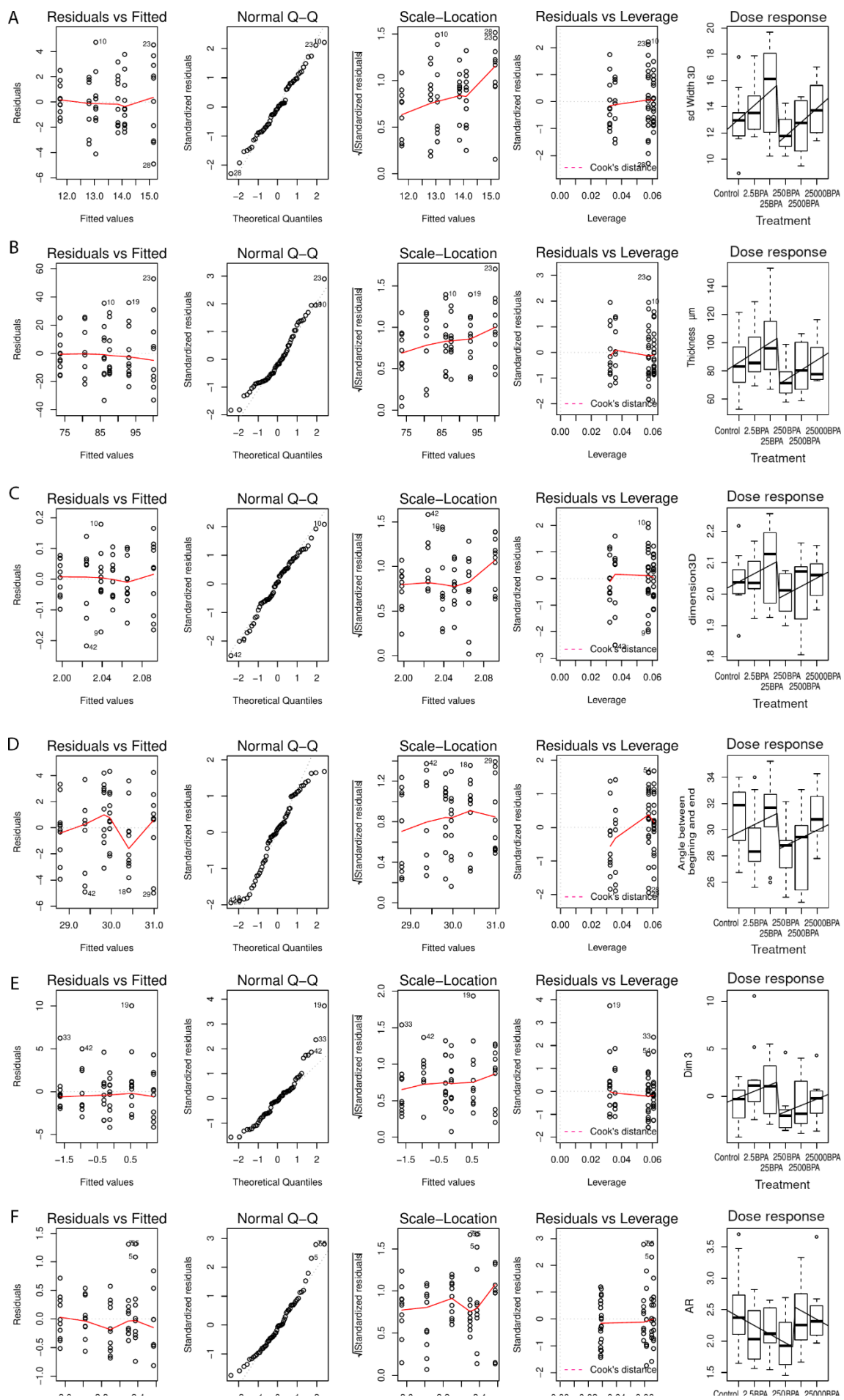
156

157 **Figure S7.** Estimated type 1 error rates on data generated by simulation (0.05 in black, 0.01 in blue,
 158 0.005 in red). A, C; the different variables are not correlated by construction. B,D: the different
 159 variables are correlated with coefficients stemming from our data. A, B: Type 1 error rate as a function
 160 of the threshold for criterion B(p_{thr}), with 20 variables. C, D: Type 1 error rate as a function of the
 161 number of features observed for $p_{\text{thr}}=0.5$.

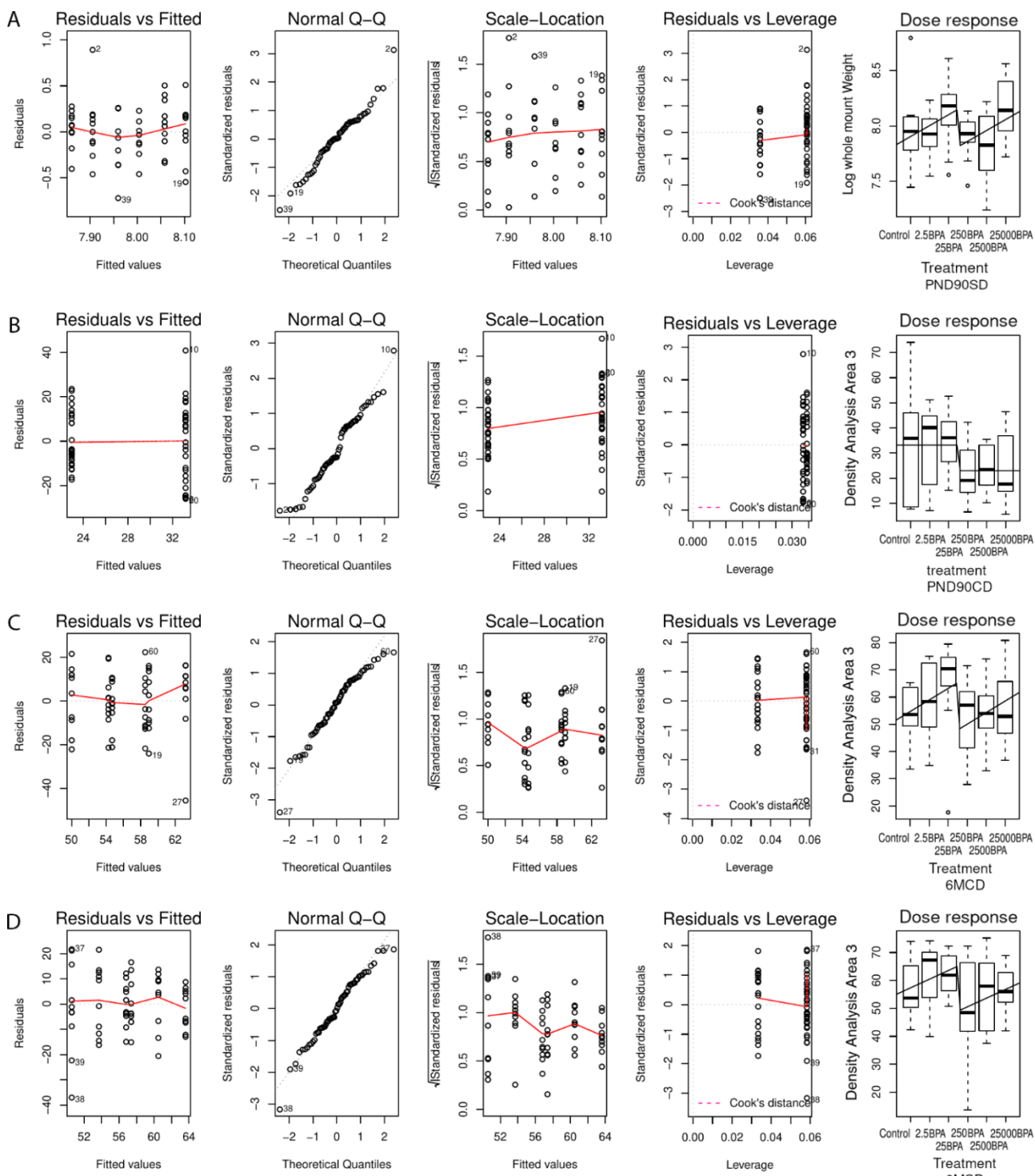


162
163
164
165
166
167
168
169

Figure S8. Estimated type 2 error rates on data generated by simulation (0.05 in black, 0.01 in blue, 0.005 in red). A, C, E: the different variables are not correlated by construction. B,D,F: the different variables are correlated with coefficients stemming from our data. A, B: type 2 error rate as a function of the threshold for criterion B(p_{thr}), with 20 variables and $a=0.6$ which is an intermediate value. C,D: type 2 error rate as a function of a with $N=20$. E, F: type 2 error rate as a function of the number N of variables describing each individual with $a=0.6$, and $p_{thr}=0.5$.



171 **Figure S9** Graphical tests to assess the quality of the regressions in PND21 animals. Control: vehicle
172 control, BPA: bisphenol A. Units: $\mu\text{g}/\text{kg}$ body weight (bw)/day. The method is provided by the lm
173 method in cran R. The first graph, Residual versus Fitted assesses the presence of a pattern not taken
174 into account by the model and homoscedasticity (i.e., that variance is constant). The second graph as-
175 sseses the normality of residuals. The third graph is used to assess homoscedasticity. The fourth graph
176 aims at assessing the presence of outliers. Last, the fifth graph displays a box plot of the data and the
177 fitted model. The midline represents the median, the box represents the quartiles above and below the
178 median and the whiskers represent the two other quartiles, excluding outliers. The features represented
179 are A sd width 3D, B Thickness, C Fractal dimension in 3D, D Angle between beginning and end
180 (here, the pattern does not fit the model completely), E Dim.3 resulting from PCA and F Aspect ratio.



184 **Figure S10.** Graphical tests to assess the quality of the regressions in 90 day and 6 month animals.
 185 The method is provided by the lm method in cran R. The first graph, Residual versus Fitted, assesses
 186 the presence of a pattern not taken into account by the model and homoscedasticity (i.e., that variance
 187 is constant). The second graph assesses the normality of residuals. The third graph is used to assess ho-
 188 moscedasticity. The fourth graph aims at assessing the presence of outliers. Last, the fifth graph dis-
 189 plays a box plot of the data and the fitted model. The midline represents the median, the box represents
 190 the quartiles above and below the median and the whiskers represent the two other quartiles, excluding
 191 outliers. The features represented are A Mammary gland weight in PND90SD, B Density in area 3 in
 192 PND90CD, C Density in area 3 in 6MCD and D Density in area 3 in 6MSD.